

## 23% efficient p-type crystalline silicon solar cells with hole-selective passivating contacts based on physical vapor deposition of doped silicon films

Di Yan, Andres Cuevas, Sieu Pheng Phang, Yimao Wan, and Daniel Macdonald

Research School of Engineering, The Australian National University, Canberra ACT 2601, Australia

(Received 25 April 2018; accepted 24 July 2018; published online 9 August 2018)

Of all the materials available to create carrier-selective passivating contacts for silicon solar cells, those based on thin films of doped silicon have permitted to achieve the highest levels of performance. The commonly used chemical vapour deposition methods use pyrophoric or toxic gases like silane, phosphine and diborane. In this letter, we propose a safer and simpler approach based on physical vapour deposition (PVD) of both the silicon and the dopant. An *in-situ* doped polycrystalline silicon film is formed, upon annealing, onto an ultrathin  $\text{SiO}_x$  interlayer, thus providing selective conduction and surface passivation simultaneously. These properties are demonstrated here for the case of hole-selective passivating contacts, which present recombination current densities lower than  $20 \text{ fA/cm}^2$  and contact resistivities below  $50 \text{ m}\Omega \text{ cm}^2$ . To further demonstrate the PVD approach, these contacts have been implemented in complete p-type silicon solar cells, together with a front phosphorus diffusion, achieving an open-circuit voltage of 701 mV and a conversion efficiency of 23.0%. These results show that PVD by sputtering is an attractive and reliable technology for fabricating high performance silicon solar cells. *Published by AIP Publishing.*

<https://doi.org/10.1063/1.5037610>

The implementation of carrier-selective passivating contacts has shown great potential for approaching the practical efficiency limit of  $\sim 27.5\%$  for silicon solar cells,<sup>1</sup> which is itself quite close to the theoretical limit of 29.5%.<sup>2</sup> A relatively simple way to fabricate such passivating contacts is to form a doped silicon film onto an ultra-thin interfacial silicon oxide layer, which permits the tunneling of electrons or holes, depending on the doping type, while helping to suppress recombination at the surface of the silicon wafer.<sup>3,4</sup> Such passivating contact structures have recently enabled the achievement of 26.1% efficient silicon solar cells<sup>5</sup> and are rapidly gaining popularity, both among research institutes and the PV industry. Commonly, the silicon films are formed by chemical vapour deposition (CVD), either plasma-enhanced (PECVD) or at low pressure (LPCVD), using gaseous precursors for the silicon (silane or dichlorosilane) and in many cases also for the dopants (diborane or phosphine).<sup>6,7</sup> The use of these gases, normally at relatively high deposition temperatures, requires elaborate safety measures, since they are extremely hazardous, which poses challenges for the mass production of solar cells.

In this letter, we propose an alternative technology to make carrier-selective passivating contacts based on the physical vapour deposition (PVD) of *in-situ* doped silicon films. The chosen PVD technique is sputtering, which can be performed at room temperature and does not involve any hazardous gases.<sup>8,9</sup> Both the silicon and an appropriate dopant element can be deposited using solid, non-toxic targets, and sputtering machines can have a smaller footprint and infrastructure than CVD ones.<sup>9–11</sup> In addition, sputtering deposition takes place only on one-side of the wafer, which is advantageous for process integration. Sputtering is widely used in the fields of microelectronics, optics and large-scale coating of glass and plastics, and has been applied commercially since

1930.<sup>8</sup> Within photovoltaics, it is commonly used in thin-film solar cell technologies (CdTe, CIGS and a-Si) and to deposit the TCO (transparent conductive oxide) layers needed for a-Si (amorphous silicon)/c-Si (monocrystalline silicon) heterojunction solar cells.<sup>8</sup> We present here the development of hole-selective passivating contacts by sputtering silicon and boron onto an ultrathin  $\text{SiO}_x$  interlayer. The main steps in the fabrication of these contacts are optimized, including the sputtering deposition conditions and the subsequent high temperature step needed to partially crystallize the film and activate the dopant. Once optimized, these PVD hole-selective contacts are applied to high performance p-type silicon solar cells in order to demonstrate the proposed method.

The main electrical parameters of a carrier-selective passivating contact are the recombination current density  $J_{oc}$  and the contact resistivity  $\rho_c$ . The former was measured with the PCD (photoconductance decay) and QSSPC (quasi-steady state photoconductance)<sup>12,13</sup> methods on symmetrically coated  $200 \mu\text{m}$  thick, (100) oriented  $100 \Omega \text{ cm}$  p-type FZ (float zone) silicon wafers (see inset in Fig. 2). The contact resistivity was measured with the Cox-Strack method<sup>14</sup> on single side coated  $200 \mu\text{m}$  thick, (100) oriented,  $0.5 \Omega \text{ cm}$  p-type CZ (Czochralski) silicon wafers (shown in Fig. 2). After a standard RCA clean and HF dip, a  $\sim 1.4 \text{ nm}$  thin chemical oxide layer was grown on silicon wafers by immersing them in hot nitric acid. Subsequently, *in-situ* boron doped silicon films were deposited in a single co-sputtering process, using an undoped silicon target (with a purity of 99.999%) and a boron target (with a purity of 99.999%) at the same time.<sup>15–17</sup> The co-sputtering process was performed at room temperature with a pressure range of 1.5 mT to 6 mT. The RF power density applied for sputtering the undoped silicon was  $\sim 3.1 \text{ W/cm}^2$ , while the RF power density was varied with a range of from  $1.9 \text{ W/cm}^2$  to

3.1 W/cm<sup>2</sup> for the boron target to obtain different dopant concentrations. After deposition, the samples were inserted into a quartz furnace at a temperature ranging from 800 °C to 980 °C, in nitrogen. This high temperature step is intentionally used to activate the dopant atoms and partially crystallize the silicon film, simultaneously.

Figure 1 shows the ECV (Electrochemical Capacitance-Voltage) profiles of electrically active boron in several PVD hole-selective passivating contact structures. As is typical of *in-situ* doped polysilicon layers, the PVD samples in Fig. 1 show constant active boron profiles with a concentration above  $1 \times 10^{20}$  cm<sup>-3</sup> in the silicon film, with a sharp drop at the location of the interfacial SiO<sub>x</sub> (indicated as dash lines in Fig. 1) and a tail of the dopant into the crystalline silicon wafer. Furthermore, the total dose of boron atoms can be easily modified by applying a different RF power to the boron target. As an example, Fig. 1 shows that a relatively low applied boron power of 1.9 W/cm<sup>2</sup> results in a lower boron concentration, whereas a higher power density of 3.1 W/cm<sup>2</sup> leads to a higher boron concentration. In terms of their recombination parameters, the sample with higher power density and heavier boron concentration ( $\sim 3 \times 10^{20}$  cm<sup>-3</sup>) yielded 10 times lower  $J_{oc}$  than the sample with the lower boron concentration ( $\sim 2 \times 10^{20}$  cm<sup>-3</sup>). Once the applied power density reached 3.1 W/cm<sup>2</sup>, their recombination did not improve further. These experiments indicate that the power density and the dopant level incorporated into the silicon film are critical factors to achieve satisfactory passivation.

The deposition conditions, therefore, play a primary role in the formation of the PVD hole-selective passivating contacts and their final performance, controlling the total dose of dopant atoms, as shown in Fig. 1, as well as the properties of the silicon film.<sup>9,11,17</sup> During deposition, the inclusion of the sputtering gas, normally Ar, can modify the microstructure of the silicon film.<sup>9,18</sup> It has been shown that high Ar pressure leads to silicon films with a high refractive index, which strongly correlates to the quality of the film<sup>9</sup> and, as we have found, with the electrical performance of the PVD

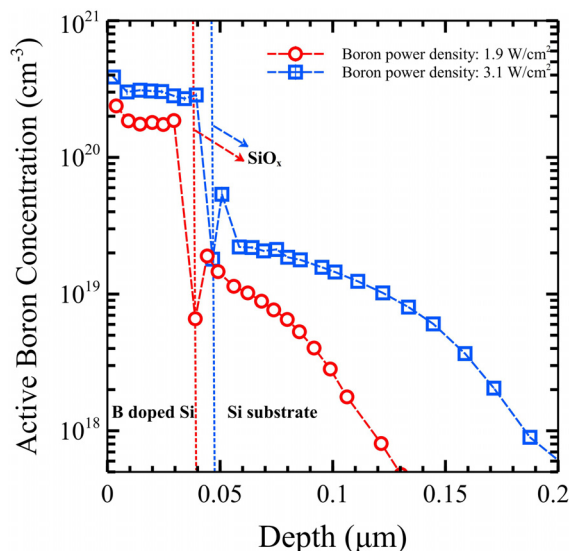


FIG. 1. ECV profiles of ionized boron atoms corresponding to PVD hole-selective passivating contacts with different boron sputtering power densities at a pressure of 2.7 mT. The annealing temperature was 900 °C for 30 min.

carrier-selective passivating contacts as well. Figure 2 shows the recombination current density  $J_{oc}$  and the contact resistivity  $\rho_c$  of the PVD hole-selective contacts as a function of the sputtering pressure. The same 70 nm as-deposited *in-situ* boron doped silicon film thickness was obtained despite the different pressures by adjusting the deposition time and applying a power density of 3.1 W/cm<sup>2</sup> to both the silicon and the boron targets. For a given power density, high pressure leads to a slower deposition rate: the latter was  $\sim 4.7$  nm/min at 1.5 mT,  $\sim 4.5$  nm/min at 2 mT,  $\sim 4$  nm/min at 2.7 mT, and  $\sim 3.4$  nm/min at 5 mT. After activation, we found that the final passivating quality and contact resistivity are strongly affected by the sputtering pressure. The lowest recombination current, ten times lower than the value obtained at a pressure of 1.5 mT, was achieved at deposition pressures higher than 2.7 mT. It is known that there is a strong correlation between the interfacial condition and the final passivation quality.<sup>7,19–21</sup> The results in Fig. 2 indicate that low pressure more easily leads to degradation of the interface, probably causing a higher density of oxide break-up sites after the high temperature activation anneal. On the other hand, the lowest contact resistivity is achieved using a low sputtering pressure, which is also consistent with a higher degree of oxide break-up. As shown in Fig. 2, PVD contacts deposited at 1.5 mT gave  $\rho_c \approx 5.2$  mΩ cm<sup>2</sup>, which is two orders of magnitude lower than the  $\rho_c$  value corresponding to 5 mT.

After the deposition of the *in-situ* boron doped silicon film, a high temperature process is required to form the hole-selective passivating contact, acting both as a re-crystallization and a dopant activation step.<sup>11,22</sup> Although the crystallinity of the films was not examined here, the activation of the boron atoms can be detected by means of sheet resistance measurements. The sheet resistance of the as-deposited PVD films was un-measurably high with a four-point probe set up,<sup>23</sup> indicating

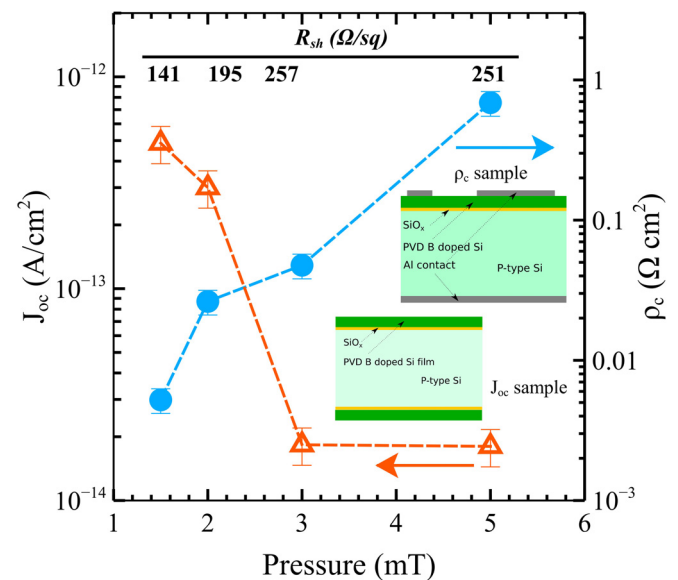


FIG. 2. Recombination current density (indicated as empty triangles) and contact resistivity (indicated as filled circles) of *in-situ* doped PVD hole-selective passivating contact as a function of sputtering deposition pressure. Their final sheet resistances values are also given. The activation process was carried at 950 °C. The different *in-situ* boron doped silicon films obtained at different pressures have a similar thickness of  $\sim 70$  nm.

negligible conductivity and a very small amount of active boron atoms in the as-deposited films.<sup>16</sup> After thermal annealing at 950 °C, the sheet resistance became measurable, with values lower than 250  $\Omega/\text{sq}$  (as indicated in Fig. 2). It has been demonstrated that a thermal process leads to the recrystallization of sputtered silicon films.<sup>9,11,24,25</sup> By controlling this thermal process, amorphous sputtered silicon can be turned into polycrystalline silicon, and this is considered the safest way of obtaining polycrystalline silicon films with improved electrical stability.<sup>9,11</sup> The higher  $\rho_c$  obtained at a high deposition pressure can also be correlated to the amount of active boron concentration in the overall Si film/ $\text{SiO}_x$ /Si substrate structure, which was evaluated through sheet resistance measurements. A higher sheet resistance (fewer dopants) was generally found for the layers deposited at a higher pressure, as labelled in Fig. 2. The final sheet resistance at pressures greater than 3 mT was almost 2 times higher than that obtained at 1.5 mT.

Figures 3 and 4 show the recombination current density  $J_{oc}$  and the contact resistivity  $\rho_c$  of PVD hole-selective passivating contacts having two different thicknesses of  $\sim 40$  nm and  $\sim 70$  nm as a function of the annealing temperature. The *in-situ* boron doped silicon films were deposited at a pressure of 2.7 mT with an applied power density of 3.1  $\text{W}/\text{cm}^2$  for both the undoped silicon and the boron targets. As has been presented previously, the interfacial conditions of the passivating contact structures strongly depend on the high temperature annealing step (including both annealing in an inert gas or a dopant diffusion process).<sup>4,7,26,27</sup> An excessively high temperature can lead to a high level of interfacial oxide break-up and a high dopant concentration in the silicon substrate, which consequently leads to poor passivation quality and good contact resistivity.<sup>4,26</sup> As shown in Figs. 3 and 4,  $J_{oc} \approx 320 \text{ fA}/\text{cm}^2$  with a very low  $\rho_c \approx 4 \text{ m}\Omega \text{ cm}^2$  has been achieved at 1010 °C for the 70 nm thick PVD contacts. Therefore, a lower temperature of 950 °C is preferable for these 70 nm thick layers, while an even lower temperature of 900 °C is optimum for the thinner 40 nm layers, since these

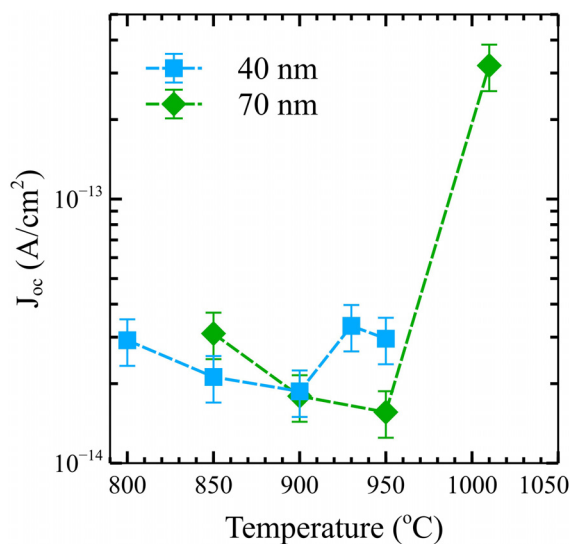


FIG. 3. Recombination current density of PVD hole-selective passivating contacts as a function of activation temperature. The as-deposited thickness of the *in-situ* boron doped silicon films was approximately 40 nm (square symbols) or 70 nm (diamond symbols).

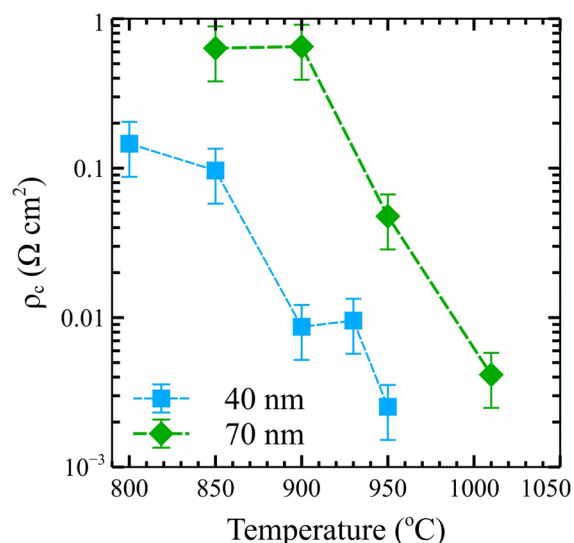


FIG. 4. Contact resistivity of PVD hole-selective passivating contacts as a function of activation temperature. The corresponding test samples were processed alongside those shown in Fig. 4.

lower temperatures enable achieving the lowest  $J_{oc}$  value together with a sufficiently low  $\rho_c$  value, as shown in Figs. 3 and 4. The fact that the optimized temperature is shifted towards a higher value for thicker silicon layers is similar to the results presented in Refs. 26 and 27. At those optimized annealing temperatures, we achieved  $J_{oc} \approx 18 \text{ fA}/\text{cm}^2$  with a contact resistivity of 8  $\text{m}\Omega \text{ cm}^2$  for a  $\sim 40$  nm PVD *in-situ* boron doped passivating contact and a  $J_{oc} \approx 16 \text{ fA}/\text{cm}^2$  with a contact resistivity of 47  $\text{m}\Omega \text{ cm}^2$  for a  $\sim 70$  nm thick one.

In order to demonstrate the passivation quality and carrier selectivity of the PVD hole-selective passivating contacts described previously, we have fabricated p-type silicon solar cells implementing them as a full area rear contact, as shown in Fig. 5. Monocrystalline FZ p-type silicon wafers with a resistivity of  $\sim 1 \Omega \text{ cm}$  and a final thickness of 200  $\mu\text{m}$  were used to form several  $2 \times 2 \text{ cm}^2$  pyramidally textured cells on each 4-inch wafer. A dual phosphorus doped region was created on the front side within the active area of the cell by thermally diffusing phosphorus from  $\text{POCl}_3$  twice: a deep and highly doped  $n^{++}$  layer under the metal fingers and a moderately doped  $n^+$  layer over the rest of the front surface, onto which a silicon nitride antireflection/passivating coating was deposited by PECVD. The PVD hole-selective passivating contacts were formed by first growing an ultra-thin ( $\sim 1.4 \text{ nm}$ )  $\text{SiO}_x$  on the wafers by hot nitric acid oxidation and then depositing a 70 nm thick silicon/boron film on the rear surface by PVD (*in-situ* doped). This 70 nm thick layer was found to be more robust and better adapted to our solar cell fabrication process than thinner layers, maintaining its passivation qualities throughout the subsequent solar cell fabrication steps, including the activation step at 950 °C, which for these thicker films is optimal, as shown in Fig. 3. The front metal grid was formed by photolithography, metal evaporation and silver plating and a  $\sim 900 \text{ nm}$  silver layer was vacuum deposited on the rear side. The finished solar cells were measured under standard testing conditions (AM1.5 solar spectrum, 25 °C) using a Sinton Instruments solar simulator and, as a reference, an n-type poly-Si contact



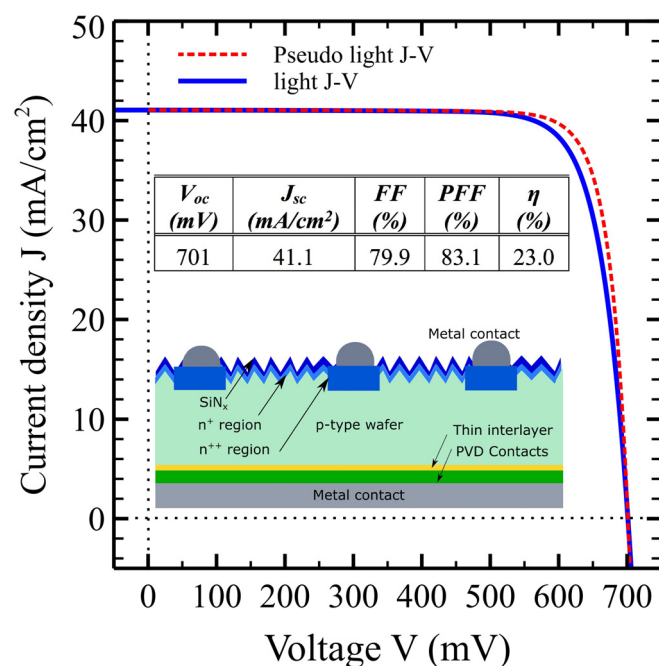


FIG. 5. Current-voltage characteristics (light J-V and pseudo-light J-V curves) of a p-type silicon solar cell with a PVD hole-selective passivating contact. Its schematic structure and output electrical parameters are shown in the same figure.

cell measured by ISFH's calibration laboratory. The performance parameters of the best p-type solar cells, which reached a 23.0% conversion efficiency, are given in Fig. 5. In this particular device, a relatively low fill factor was obtained, due to a high series resistance of  $\sim 0.6 \Omega \text{ cm}^2$ , which resulted from an excessively light phosphorus diffusion at the front, rather than resistive losses on the rear side (a separate batch with a heavier phosphorus diffusion achieved a higher fill factor of 82.3%). The series resistance was extracted from a comparison between the J-V curve under illumination and the pseudo light J-V curve, obtained by measuring the open-circuit voltage as a function of light intensity.<sup>28</sup> The latter curve, which is not affected by series resistance, gives a pseudofill factor (PFF) of 83.1, which implies that the conversion efficiency without series resistance would be 23.9%. Thus, there is an ample room for further improvement of these p-type silicon solar cells, including the possibility of further gains in  $J_{sc}$  and  $V_{oc}$ . The average efficiency of all the cells in the 4-inch wafer was 22.5%, indicating excellent uniformity of the PVD passivating contact technique.

The experimental results presented in this letter demonstrate that PVD offers an attractive technological option for fabricating the next generation of high performance silicon solar cells. It is a simple, safe and reproducible approach for the formation of high quality carrier-selective passivating contacts on silicon wafers. It is suitable for *in-situ* doping and single-side deposition, without the requirement of a separate doping process, such as thermal diffusion or ion implantation. In this letter, we have shown that it can be used to fabricate high performance full area hole-selective passivating contacts and p-type silicon solar cell devices. The PVD technique can also be applied to fabricate electron-selective contacts and its further optimisation can be

expected to lead to even higher efficiency devices than those presented here.

We gratefully acknowledge the support of The Australian National University and University of Canberra through the Discovery Translation Fund 2.0, managed by ANU Connect Ventures. Additional support was received from the Australian Renewable Energy Agency (ARENA) through the Solar PV Research and Development Programme—Project AC/000001 and via the Australian Centre for Advanced Photovoltaics (ACAP).

- <sup>1</sup>K. Yoshikawa, H. Kawasaki, W. Yoshida, T. Irie, K. Konishi, K. Nakano, T. Uto, D. Adachi, M. Kanematsu, and H. Uzu, *Nat. Energy* **2**, 17032 (2017).
- <sup>2</sup>A. Richter, M. Hermle, and S. W. Glunz, *IEEE J. Photovoltaics* **3**(4), 1184–1191 (2013).
- <sup>3</sup>F. Feldmann, M. Bivour, C. Reichel, M. Hermle, and S. W. Glunz, *Sol. Energy Mater. Sol. Cells* **120**(Part A), 270–274 (2014).
- <sup>4</sup>U. Römer, R. Peibst, T. Ohrdes, B. Lim, J. Krügener, E. Bugiel, T. Wietler, and R. Brendel, *Sol. Energy Mater. Sol. Cells* **131**, 85–91 (2014).
- <sup>5</sup>F. Haase, C. Klamt, S. Schafer, A. Merkle, M. Rienacker, J. Krügener, R. Brendel, and R. Peibst, paper presented at the 8th SiliconPV 2018, Lausanne, Switzerland, 2018.
- <sup>6</sup>Y. Tao, E. L. Chang, A. Upadhyaya, B. Roundville, Y.-W. Ok, K. Madani, C.-W. Chen, K. Tate, V. Upadhyaya, F. Zimbardi, J. Keane, A. Payne, and A. Rohatgi, Paper presented at the 2015 IEEE 42nd Photovoltaic Specialist Conference (PVSC), 2015.
- <sup>7</sup>F. Feldmann, M. Simon, M. Bivour, C. Reichel, M. Hermle, and S. W. Glunz, *Appl. Phys. Lett.* **104**(18), 181105 (2014).
- <sup>8</sup>R. A. Levy, *Microelectronic Materials and Processes* (Springer Science & Business Media, 2012).
- <sup>9</sup>T. Voutsas, H. Nishiki, M. Atkinson, J. Hartzell, and Y. Nakata, *SHARP Tech. J.* **80**(3), 36–42 (2001).
- <sup>10</sup>T. Abe and M. L. Reed, paper presented at the IEEE, The Ninth Annual International Workshop on Micro Electro Mechanical Systems, 1996, MEMS'96, Proceedings. An Investigation of Micro Structures, Sensors, Actuators, Machines and Systems, 1996.
- <sup>11</sup>Z. Sun, K. Tong, and W. Lee, *Thin Solid Films* **288**(1–2), 224–228 (1996).
- <sup>12</sup>R. A. Sinton and A. Cuevas, *Appl. Phys. Lett.* **69**(17), 2510–2512 (1996).
- <sup>13</sup>D. E. Kane and R. M. Swanson, in *IEEE Photovoltaic Specialists Conference* (1985).
- <sup>14</sup>R. H. Cox and H. Strack, *Solid-State Electron.* **10**(12), 1213–1218 (1967).
- <sup>15</sup>M. de Lima, Jr., F. Freire, Jr., and F. Marques, *Braz. J. Phys.* **32**(2A), 379–382 (2002).
- <sup>16</sup>Y. Ohmura, M. Takahashi, M. Suzuki, N. Sakamoto, and T. Meguro, *Physica B* **308**, 257–260 (2001).
- <sup>17</sup>X. Zhang, Ph.D. thesis, "Sputtered aluminium oxide and amorphous silicon for silicon solar cells," The Australian National University, 2015.
- <sup>18</sup>H. F. Winters and E. Kay, *J. Appl. Phys.* **38**(10), 3928–3934 (1967).
- <sup>19</sup>D. Yan, A. Cuevas, Y. Wan, and J. Bullock, *Phys. Status Solidi RRL* **9**(11), 617–621 (2015).
- <sup>20</sup>J. L. Egle and J. L. Gray, *IEEE Trans. Electron Devices* **38**(9), 2112–2117 (1991).
- <sup>21</sup>A. A. Eltoukhy and D. J. Roulston, *IEEE Trans. Electron Devices* **29**(12), 1862–1869 (1982).
- <sup>22</sup>T. Serikawa, "Rapid isothermal annealing of sputtered phosphorus-doped silicon films," *J. Electrochem. Soc.* **133**, 447 (1986).
- <sup>23</sup>W. Wang, J. Huang, W. Xu, J. Huang, Y. Zeng, and W. Song, *J. Mater. Sci.: Mater. Electron.* **24**(6), 2122–2127 (2013).
- <sup>24</sup>P. P. Altermatt, J. Schmidt, G. Heiser, and A. G. Aberle, *J. Appl. Phys.* **82**(10), 4938–4944 (1997).
- <sup>25</sup>D. Y. Kim, H. S. Cho, K. B. Park, J. Y. Kwon, J. S. Jung, and T. Noguchi, *J. Korean Phys. Soc.* **45**, S847–S850 (2004).
- <sup>26</sup>D. Yan, A. Cuevas, J. Bullock, Y. Wan, and C. Samundsett, *Sol. Energy Mater. Sol. Cells* **142**, 75 (2015).
- <sup>27</sup>D. Yan, A. Cuevas, Y. Wan, and J. Bullock, *Sol. Energy Mater. Sol. Cells* **152**, 73–79 (2016).
- <sup>28</sup>R. Sinton and A. Cuevas, Presented at the Proceedings of the 16th European Photovoltaic Solar Energy Conference, Glasgow, UK, 2000.